Available online at www.sciencedirect.com
SCIENCE DIRECT®
Carbohydrate Research 340 (2005) 981–988
Carbohydrate RESEARCH

The complex of xylan and iodine: the induction and detection of nanoscale order

Xiaochun Yu[a] and Rajai H. Atalla[a,b,*]

[a]*Department of Chemical and Biological Engineering, University of Wisconsin, Madison, WI 53726, USA*
[b]*USDA, Forest Products Laboratory, One Gifford Pinchot Dr., Madison, WI 53726, USA*

Received 28 October 2004; accepted 25 January 2005

Dedicated to Professor David A. Brant

Abstract—The complex of xylan and iodine and its formation in a solution of xylan, $CaCl_2$, and I_2 + KI was investigated by UV/Vis, second-derivative UV/Vis, and Raman spectroscopy. The complex forms only at very high concentrations of $CaCl_2$, suggesting that when the water available in the solution is not sufficient to fully hydrate the calcium cation the chelation with the hydroxyl groups of the xylan can occur. The electronic spectra indicate that iodine is present in the form of three linear polyiodides I_9^{3-}, I_{11}^{3-}, and I_{13}^{3-} structures, which the Raman spectra show to be linear aggregates of the I_3^- and I_5^- substructures. Iodide concentration has a significant influence on the relative population of I_9^{3-}, I_{11}^{3-}, and I_{13}^{3-}, as well as I_3^- and I_5^-, which lead to changes in both the UV/Vis absorption maxima shifts and changes in the Raman spectra. The key difference between this system of complexes with the linear polyiodide aggregates and that of amylose is that the longest aggregate observed with the amylose system, the I_{15}^{3-} polyanion, is not observed with the xylans. This indicates that the ordered arrays in the xylan–iodine complex do not exceed 4 nm in length. It is not possible to conclude at this time whether the ordered segment of the xylan molecule is linear or helical. If it is linear the length of the longest ordered arrays would be eight xylose residues. The number would exceed eight if the xylan molecule were helically wound. Published by Elsevier Ltd.

Keywords: Xylan; Polyiodide; Xylan–iodine complex; Nanoscale order

1. Introduction

Solutions of iodine and iodides have long been used as stains to facilitate the identification of cellulosic fibers with respect to source and processes of isolation.[1] A number of formulations have been used, either in water or in salt solutions,[1,2] but they all rely on the differential color reaction of the plant cell-wall polysaccharides with iodine. Although the formulations were devised completely empirically, they present very subtle color differences among different fibers. For example, Graff 'C' stain presents fiber color from blue to red to yellow.[2,3] These color variations point to subtle differences in structure among different fibers. In an effort to understand the underlying mechanisms we have carried out a number of studies of the iodine complexes with polysaccharides. The first effort was focused on understanding the nature of the polyiodide structures responsible for the color[4] and relied on the much investigated amylose–iodine complex system. Here we report on extension of our investigation to the complexes of iodine with xylans.

Our previously reported studies of the amylose–iodine complex in solution[4] established a foundation for extending the studies of iodine complexes to those with the cellulose and the hemicelluloses. With the amylose system, our investigation focused on the organization of polyiodide chains in the amylose–iodine complex. We relied on complementary observations of Raman spectra, UV/Vis, and second derivative UV/Vis

* Corresponding author. Tel.: +1 608 231 9443; fax: +1 608 231 9262; e-mail: rhatalla@facstaff.wisc.edu

0008-6215/$ - see front matter Published by Elsevier Ltd.
doi:10.1016/j.carres.2005.01.029

spectroscopies complemented by semi-empirical calculations based on a simple structural model. The Raman spectra indicated that the primary substructures of the polyiodide chains are I^{3-} and I^{5-} subunits. The second derivatives of the UV/Vis spectra revealed four absorption peaks, which were attributed to the four polyiodide species I_9^{3-}, I_{11}^{3-}, I_{13}^{3-}, and I_{15}^{3-}, on the basis of AM1 calculations and a polyiodide structural model. In an amylose–iodine–iodide solution, the polyiodides within the amylose helices exist in equilibrium with iodine and iodide. Changing the iodide concentration causes changes in the relative population of the different polyiodide chains and their substructures. The change in population of polyiodide species is accompanied by a corresponding shift in the positions of the UV/Vis absorption maxima. The Raman spectra reflect parallel changes in the population of the I^{3-} and I^{5-} subunits. Our findings regarding polyiodide chainlengths are consistent with previously reported observations concerning the changes in the color characteristics of the iodine–amylose complexes, with the length of the amylose molecule up to a DP between 40 and 50.

Here we turn our attention to birch xylan. This is motivated by the observations in the early 1960s that xylans with linear structures or with limited branching can form a blue complex with iodine in concentrated $CaCl_2$ solution.[5–7] In particular it was shown that all of the xylans tested that were predominantly linear do form solution complexes with the $CaCl_2$ and I_2 + KI system. The salts of other group II cations such as $ZnCl_2$, $MgCl_2$, or $SrCl_2$, may replace $CaCl_2$ in the reaction, but the alkali metal chlorides cannot. In salt-free solution, the reaction does not occur.[8,9] In[9] it was also shown that the primary prerequisite was four β-1→4 linkages in sequence. With the *xylo*-oligosaccharides a DP of 4 was inadequate but DPs of 5 and 6 did form the complex in $CaCl_2$ and I_2 + KI solutions. Qualitative analysis showed that xylan, $CaCl_2$, and iodine are present in the blue complex, and linear iodine arrays similar to those in the starch–iodine complex were assumed to be responsible for the color formation.[8,9] However, questions concerning the nature and structure of these iodine arrays and the influence of solution conditions on the formation of the arrays and the xylan–iodine complexes remained unresolved.

Again in this work, we relied on orchestrated use of UV/Vis, second derivative UV/Vis, and Raman spectroscopies to investigate the influence of the variables on the polyiodide systems responsible for the colors. Birch wood xylan was chosen as the representative xylan because of its linear structure and its ready availability. It is important to note here that we are introducing two new variables associated with the need for $CaCl_2$ in order for the complexes to form. The Ca^{2-} cation appears to be essential to stabilize an ordered linear configuration that can be the substrate for the extended polyiodide ions, and the Cl^- anions can enter into the equilibria of the iodide–iodine system.

2. Results

2.1. UV/Vis spectroscopy

The formation of xylan–iodine complexes requires xylan–I_2, I^-, and $CaCl_2$. In concentrated $CaCl_2$ solutions, xylan, and the polyiodides form a blue complex when the iodide concentration is low, but at high iodide concentrations, the complex turns violet. This effect of KI concentration on the xylan–iodine complex formation was examined by UV/Vis spectroscopy, and the results are shown in Figure 1.

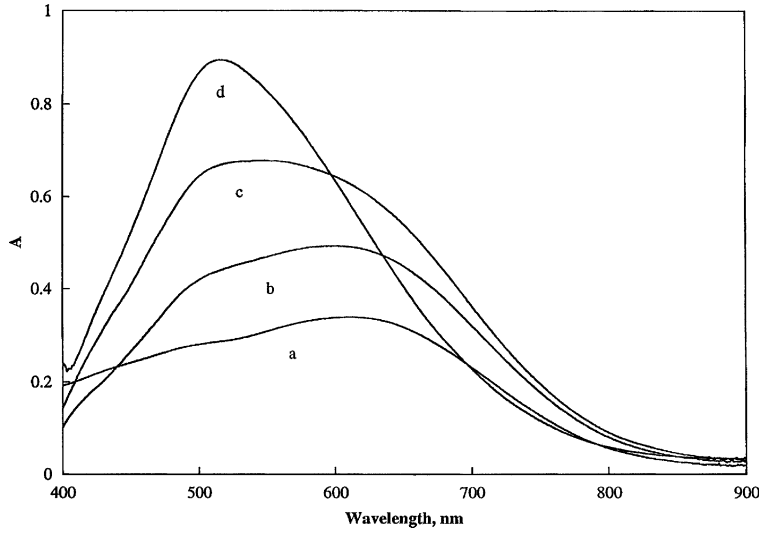

Figure 1. UV/Vis spectra of xylan–iodine complexes. Xylan concn: 0.005%; iodine concn: 0.05%; $CaCl_2$ concn: 40%. (a) 0% KI; (b) 0.1% KI; (c) 0.5% KI; (d) 5.0% KI.

UV/Vis spectra of the xylan–iodine complex at zero or low KI concentrations show a broad and asymmetrical UV/Vis absorption with a maximum at 610 nm and a shoulder around 490 nm. Small variations in KI concentration cause dramatic changes in both the shape and intensity of the UV/Vis spectra. With increasing iodide concentration, the absorption maximum position shifts toward shorter wavelengths. When the concentration of KI is increased to 5%, the absorption maximum shifts to the position of the shoulder at 490 nm so that only one absorption maximum can be observed. As the absorption maximum position shifts, the overall absorption intensity also increases.

Since the normal absorption UV/Vis spectra are broad and asymmetrical, and appear to be composed of several overlapping peaks that are difficult to resolve, the second-derivative spectra[10,11] were analyzed. With second-derivative spectra, the positions of the maximum negative curvature correspond to peaks in the original spectra. The second derivatives of the UV/Vis absorption spectra are shown in Figure 2.

The second-derivative UV/Vis spectra indicate that at low iodide concentrations, the UV/Vis spectra consist of three peaks with their maxima at approximately 495, 590, and 640 nm. With changing iodide concentration, the position of the three peaks does not shift significantly, but their relative intensities change dramatically. With increasing iodide concentration, the peaks at 590 and 635 nm decline in intensity while the peak at 495 nm is notably enhanced. At high iodide concentrations such as 5% KI, the peaks at 590 and 640 nm are too weak to identify while the peak at 495 nm becomes dominant. It appears that the position shift observed in the UV/Vis absorption spectra is the result of the relative intensity change of the three absorption peaks.

The presence of three absorption peaks in the UV/Vis spectra and their relative intensity change with increasing iodide concentration suggests that there may be at least three polyiodides in the xylan–iodine complex. The polyiodide corresponding to the UV/Vis absorption at 495 nm is favored by high iodide concentrations, while the polyiodides with UV/Vis absorption maxima at 590 and 640 nm are favored by low iodide concentrations.

The concentration of $CaCl_2$ also has a significant influence on xylan–iodine complex formation but it affects only the color intensity, since the color of the xylan–iodine remains unchanged. UV/Vis absorption measurements at 610 nm indicate that decreasing the $CaCl_2$ concentration dramatically reduces the xylan–iodine absorption. When the $CaCl_2$ concentration is below 25%, no color reaction occurs, and the UV/Vis absorption measurement indicates no absorption at all, as shown in Figure 3. This suggests that, as previously reported, concentrated $CaCl_2$ solution is necessary for the xylan–iodine complex formation.[5,6]

So far we have focused on steady-state effects that are analogous to the observations with the amylose–iodine system. However, in the instance of the xylans and the $CaCl_2$ system, there are also some kinetic effects that must be considered. They appear to be associated with the role of the $CaCl_2$ in the formation of the complexes. And these effects involve two different factors. The first is obvious from the requirement of high concentrations of $CaCl_2$ or the chloride of some other group II cation to stabilize and ordered conformation of xylan that can provide a substrate for the polyiodide ions to form an extended linear array. The second is likely associated with the reactions of the Cl^- anion with the polyiodide and iodine systems. These effects are shown in Figure 4.

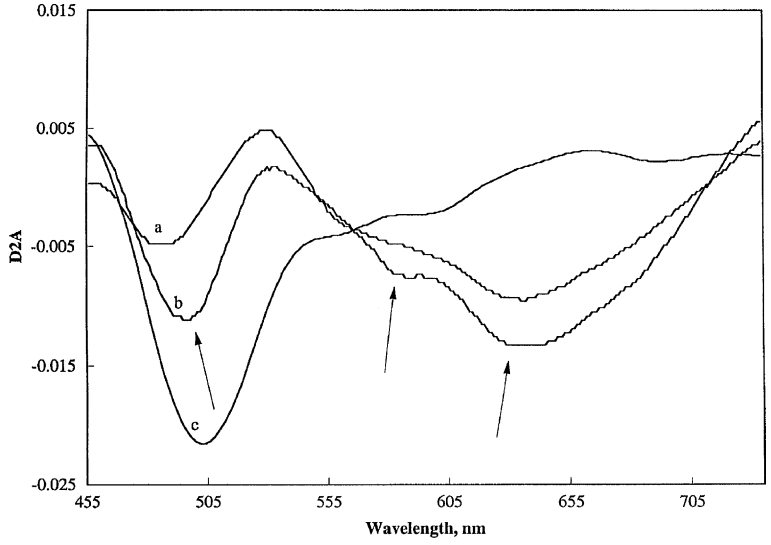

Figure 2. Second-derivative UV/Vis spectra of the xylan–iodine complex. Xylan concn: 0.005%; iodine concn: 0.05%; $CaCl_2$ concn: 40%. (a) 0% KI; (b) 0.1% KI; (c) 5.0% KI.

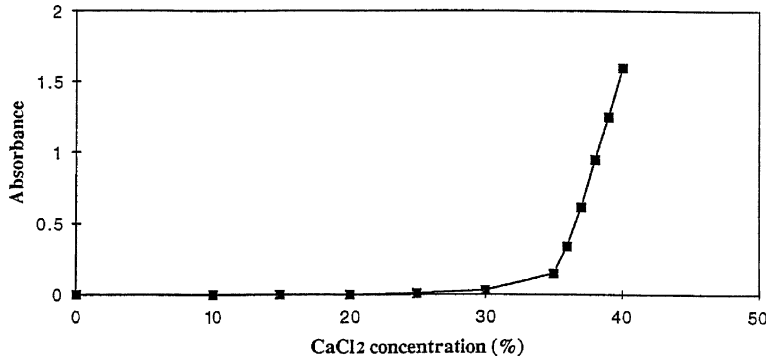

Figure 3. Influence of $CaCl_2$ concentration on the xylan–iodine complex formation. Xylan concn: 0.005%; iodine concn; 0.05%; KI concn: 0.1%.

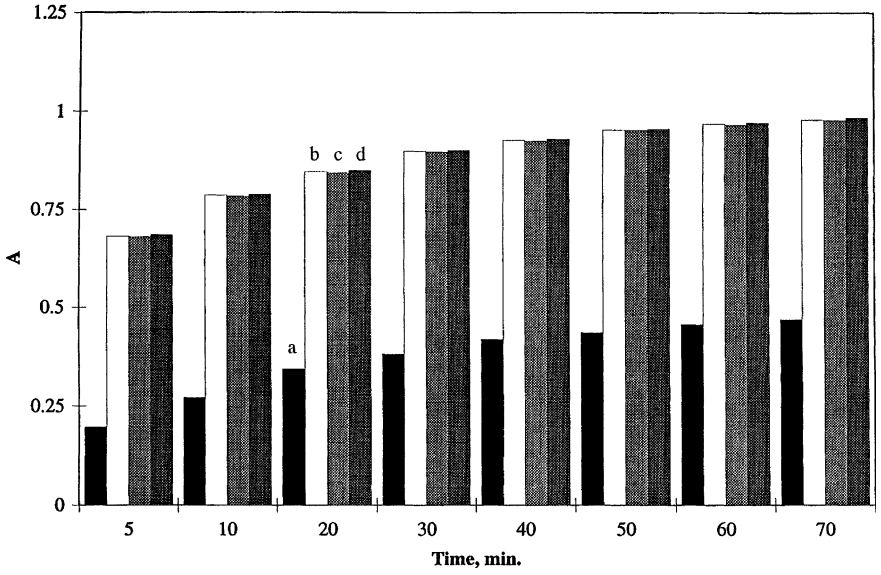

Figure 4. Influence of mixing sequence on the xylan–iodine complex formation. (a) Mixing I_2 + KI and $CaCl_2$ first and adding xylan 2 h later. (b) Mixing I_2 + KI and xylan first and adding $CaCl_2$ 2 h later. (c) Mixing $CaCl_2$ and xylan first and adding I_2 + KI 2 h later. (d) Mixing I_2 + KI, xylan and $CaCl_2$ all together at the same time.

Figure 4 shows that when $CaCl_2$ and I_2 + KI are mixed first, and the mixture allowed to stand for 2 h before xylan was added, the UV/Vis absorption intensity of the solution was much less than when the solutions were mixed in other sequence, such as, mixing $CaCl_2$ and xylan first, I_2 + KI and xylan first, or $CaCl_2$, xylan, and I_2 + KI at the same time. This indicates that the reaction between $CaCl_2$ and I_2 + KI inhibits the xylan–iodine complex formation.

It is known that both iodide and chloride can form a complex with iodine as shown in the following equilibria:[12]

$$I_2 + I^- \rightleftharpoons I_3^- \quad \text{(I)}$$

$$I_2 + Cl^- \rightleftharpoons I_2Cl^- \quad \text{(II)}$$

$$I_3 + Cl^- \rightleftharpoons I_2Cl^- + I^- \quad \text{(III)}$$

In an I_2 + KI solution, equilibrium I is present; when $CaCl_2$ is added, reactions II and III occur. These reactions reduce I_2 and I_3^- concentration in the solution, in the UV/Vis spectra of I_3^-, which has UV/Vis absorption maxima at 287 and 353 nm (Fig. 5), the UV/Vis absorption intensity of I_3^- reduces as expected.

The unusual phenomenon is that the I_3^- concentration decreases slowly. This suggests that the foregoing reactions are slow processes. After mixing $CaCl_2$ and I_2 + KI and allowing the reactions to proceed for 2 h, the concentrations of both the I_2 and I_3^- decline significantly. Thus when xylan is added, the levels of I_2 and I_3^- available for xylan–iodine complex formation are lower, and consequently less of the complex is formed.

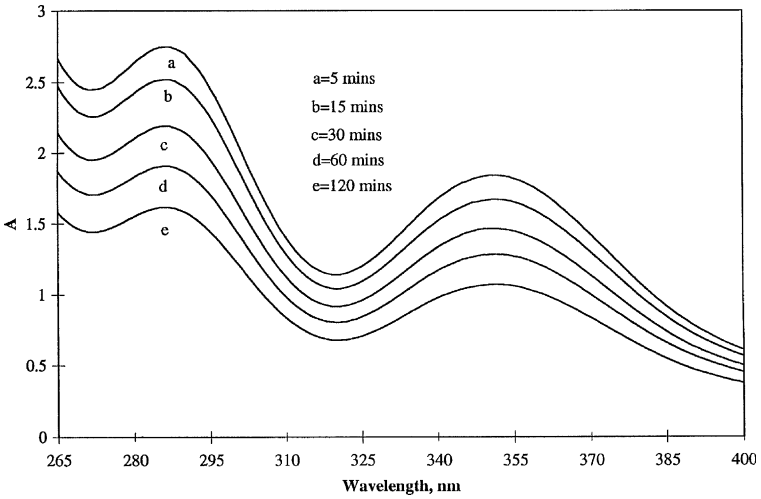

Figure 5. I_3^- concentration decreased after $CaCl_2$ was added to I_2 + KI solution.

This implies that the chloride ion in the medium inhibits xylan–iodine complex formation by competitively reacting with and consuming iodine in the solution. It also indicates that the concentrations of I_2 and I_3^- play important roles in controlling the rate of xylan–iodine complex formation.

Equilibrium III also indicates that with increasing iodide concentration, the equilibrium will shift to the left, and the I_3^- concentration will be expected to increase. This may be why increasing the KI concentration brings a dramatic intensity increase for the UV/Vis absorption of the xylan–iodine complex at 490 nm as shown in Figure 2.

In addition, Figure 4 also shows that for all the mixing sequences, the UV/Vis absorption intensity increased rapidly in the first 5 min, after that, UV/Vis absorption intensity increased gradually with increasing reaction time after all components were added, no maximum absorption was observed in 90 min. The reason is that when xylan, $CaCl_2$, and I_2 + KI were mixed, formation of xylan–iodine complex quickly consumed the available I_2 and I_3^-. But the reaction did not stop at this point because the decline in concentration of I_2 and I_3^- caused equilibria II and III to shift to the left, which produced more I_2 and I_3^-. Since the shifts of equilibria II and III are slow processes, which slowly produce I_2 and I_3^-, the result is gradual formation of additional xylan–iodine complex.

As just discussed, concentrated $CaCl_2$ solutions are necessary for the formation of the xylan–iodine complex, but the chloride anion seems to inhibit its formation. This implies that the calcium cation plays a key role in facilitating the xylan–iodine complex formation. The most plausible rationalization of this observation is that calcium forms a complex with xylan and stabilizes a linearly ordered structure. Willams and Atalla[13,14] have shown that the calcium ion has unusually strong tendency to enter into chelation with saccharides and their analogs through their vicinal hydroxyl groups. The work of Angyal[15] suggested that three adjacent hydroxyl groups in axial–equatorial–axial configuration are prerequisites for formation of complexes with carbohydrates, but Richards and Williams[16] found the prerequisites to be a minimum of three adjacent hydroxyl groups without the configuration constraint. Subsequent crystallographic studies of the calcium complex with xylose by Richards[17] revealed that the complex requires only two adjacent hydroxyl groups.

2.2. Raman spectroscopy

Raman spectroscopy was used to investigate the identity of iodine components in the xylan–iodine complex. The most sensitive range of Raman spectra for the characterization of the iodine–iodide system speciation is in the low-frequency spectral region of 25–250 cm^{-1}, which involves mainly the I–I stretching vibrations. The Raman spectra of different polyiodides in this range have been widely investigated.[18–24] It is shown that the most characteristic signal is the symmetrical I–I stretching vibration mode: for I_2 it is above 180 cm^{-1}, for I_3^- it is around 110 cm^{-1} and for I_5^- it is around 160 cm^{-1}. Although a weak signal at around 110 cm^{-1} was also found in some I_5^- samples; according to theoretical calculations and infrared spectral evidence, this signal belongs to the impurity of I_3^- and not to I_5^-.[19,22] Other polyiodides are generally composed with the three subunits noted.

Raman spectra of xylan–iodine complex formed under different conditions are shown in Figure 6. It shows that xylan–iodine complex formed in saturated iodine solution without added KI, has a very strong signal at around 160 cm^{-1} and a weak signal at around 110 cm^{-1}. When the blue xylan–iodine complex is

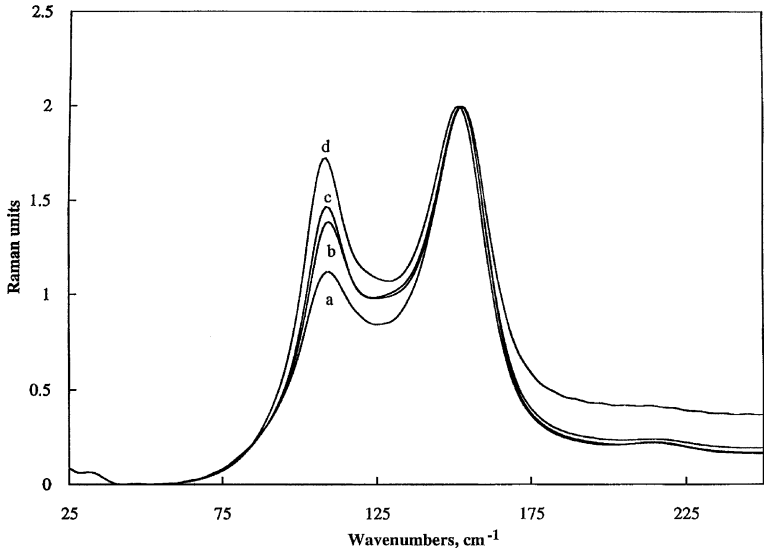

Figure 6. Raman spectra of the xylan–iodine complex. (a) From saturated iodine solution without added KI. Raman spectrum was recorded immediately after separation. (b) Exposed to air for 10 h. (c) Exposed to air for 20 h. (d) Under vacuum for 20 h.

exposed to air or placed under vacuum, its Raman spectrum change dramatically, as the band at 160 cm^{-1} is reduced in intensity while the band at 110 cm^{-1} becomes more intense. This is interpreted in terms of the slow evaporation of I_2 so that only I_3^- substructures remain.

The relative intensity of the two peaks at 110 and 160 cm^{-1} is also very sensitive to the KI concentration (Fig. 7). With increasing iodide concentration, the intensity of the peak around 160 cm^{-1} declines while the peak at around 110 cm^{-1} enhances dramatically, at KI concentration of about 1.0%, the peak around 160 cm^{-1} becomes only a shoulder; further increasing KI concentration makes this shoulder so weak that it is barely identifiable. Accompanying the relative intensity change, there is also a small position shift for the band around 160 cm^{-1}. With increasing iodide concentration, the intensity of this band is reduced dramatically, and its position shifts a little toward lower frequency. The decline in intensity is likely due to a decline in the polarizability as the polarity of the system is increased.

Meanwhile, at high iodide concentration, a shoulder at around 125 cm^{-1} and a very weak peak at 216 cm^{-1} can also been seen.

The appearance of two signals at 160 and 110 cm^{-1} in the Raman spectra of the xylan–iodine complex formed at low iodide concentration solution suggests that I_3^- and I_5^- are present in the xylan–iodine complex; the absence of signal above 180 cm^{-1} suggests that there are no discrete iodine molecules present in the xylan–iodine complex. The iodide used for the I_3^- and I_5^- formation

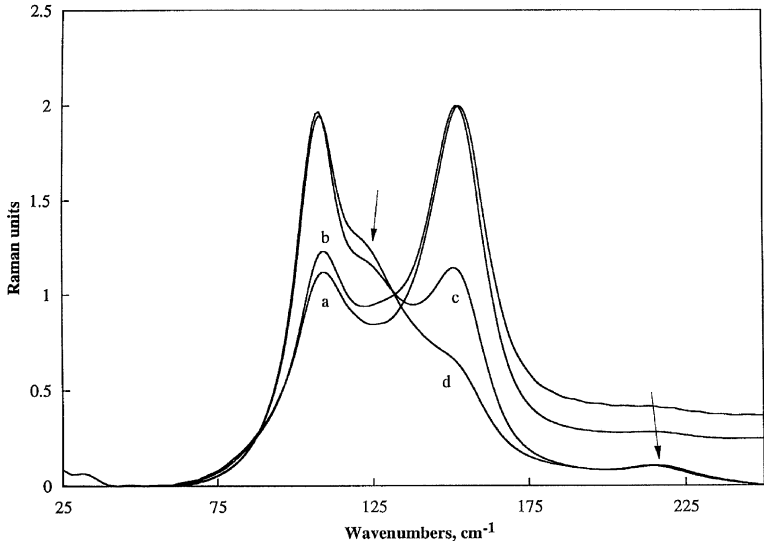

Figure 7. Raman spectra of xylan–iodine complex precipitated from solution with different iodide concentration (a) 0.0% KI; (b) 0.1% KI; (c) 0.5% KI; (d) 5% KI.

does not need to be externally added, the following iodine hydrolysis reactions also produce iodide ions:[25]

$$I_2 + H_2O \rightleftharpoons I^- + H^+ + HOI \quad (IV)$$

$$3I_2 + 3H_2O \rightleftharpoons IO_3^- + 5I^- + 6H^+ \quad (V)$$

$$I_2 + H_2O \rightleftharpoons H_2OI^+ + I^- \quad (VI)$$

When exposing the xylan–iodine complex to air or vacuum, I_5^- readily dissociates to lose I_2 and is converted to I_3^-. The observed intensity decline at 160 cm^{-1} and intensity increase at 110 $cm^{-1}$are a consequence. Increasing iodide concentration to higher levels readily converts more of the I_5^- into I_3^-; at high iodide concentration, the I_5^- subunits are completely converted into I_3^-.

Accompanying the relative intensity change was a small position shift for the band at 160 cm^{-1}. This suggests that I_3^- and I_5^- are not completely separated, the shift toward low frequency with increasing iodide concentration indicates an increase of the negative charge on the polyiodide.

At high iodide concentration, the signal at 110 cm^{-1} is very strong and becomes the dominant signal. In addition, a shoulder around 125 cm^{-1} and a peak at 216 cm^{-1} appear. The weak peak at 216 cm^{-1} is apparently the overtone of the strong signal at 110 cm^{-1} and can easily be attributed to I_3^-. The signal at 125 cm^{-1} is associated with the antisymmetrical vibration of I_3^- as noted in several reports.[20,21] One rationalization is based on possibility that the structure of I_3^- polyanion may be linear and distorted with the two I–I bonds unequal length. When the structure of I_3^- is linear with two equal length bonds, its symmetrical stretching vibration is Raman active while the antisymmetrical stretching vibration is Raman inactive. But when the two I–I bonds are unequal length, the antisymmetrical stretching vibration can become Raman active.[20] However, it also may be that the point symmetry of the isolated molecule, with equal bonds, is significantly perturbed by an association with substructures that are not equally symmetric. This antisymmetrical stretching vibration signal has been observed for several compounds at the position around 130 cm^{-1},[20,21] we assumed that the signal at 125 cm^{-1} in the xylan–iodine complex belongs to the antisymmetrical vibration of I_3^-. With serious perturbation of its point group symmetry, a relatively strong antisymmetrical stretching vibration is expected.[20] As xylan–iodine complex presents only a very weak shoulder signal, we believe the perturbation of the symmetry of I_3^- is not severe.

2.3. I_2/I^- ratio in the xylan–iodine complex

The precipitate of xylan–iodine complex formed in saturated iodine solution without added KI was separated by centrifugation and washed with $CaCl_2$ solution. This precipitate was subjected to I_2/I^- ratio analysis. The precipitate was first extracted with cyclohexane, which dissolves the I_2 and thus extracts it from the aqueous medium. After several extractions and separations, the water phase became colorless. The iodide remaining in the water phase was then oxidized with H_2O_2 into iodine and extracted again with cyclohexane. The iodine concentration in both extractions was analyzed with UV/Vis measurement, and in this manner the I_2/I^- ratio in the xylan–iodine complex was calculated and found to be 1.47.

3. Discussion

The key difference between the xylan–iodine complexes and the amylose–iodine complexes described in our previous report[4] is that concentrated $CaCl_2$ solution is a prerequisite for their formation. It is clear from Figure 3 that a sharp increase in complex formation occurred between 35% and 40% concentrations of $CaCl_2$. The sharp increase is reminiscent of the sharp increase in mercerizability of celluloses when insufficient water is available to completely hydrate the sodium cations. By analogy, we speculate that the effect of the presence of $CaCl_2$ becomes significant when there is no longer enough water to completely hydrate the calcium cations. At this point it appears that the hydroxyl groups of the xylan begin to chelate with incompletely hydrated calcium cations. Thus it is plausible to assume that such an effect is occurring. The unusual feature is that this chelation results in ordering of segments of the xylan molecules into configurations that are capable of forming charge-transfer complexes with the polyiodides. Thus such an ordering is induced by the $CaCl_2$ at the high concentrations.

The other key observation is that at very low iodide concentrations or no iodide, the longest polyiodide ion aggregates are more stable. And these reveal a key difference between the amylose and xylan system. In the amylose system the longest polyiodide aggregate was the I_{15}^{3-}, which corresponds to an absorption band that is not observed at all in the xylan–iodine complexes. The longest wavelength band observed in the xylan–iodine complex system is the I_{13}^{3-} polyanion. Based on the calculations presented in our previous report,[4] we estimate the length of the I_{13}^{3-} aggregate polyanion to be 4 nm. If the array of xylose residues is linear, this dimension would correspond to a segment that is 8 units long, assuming as in cellulose approximately 1 nm per xylobiose segment. Our results however cannot at this point exclude the possibility that a helical array of xylose residues is formed as suggested by Gaillard.[5,7] We are currently investigating complex formation between the iodine, KI, and cellulose system and the formation of charge-transfer complexes with the polyiodides in the

presence of CaCl. In that system ordering is induced by the $CaCl_2$ system and a helical conformation is not likely. That may shed further light on the nature of the ordered arrays.

4. Experimental

Material: Xylan from birch wood was purchased from Sigma. Its xylan content was >90%, and it was used without further treatment.

Stock xylan solution was prepared as follows: 0.1 g xylan was dissolved in 2 mL 1 N NaOH solution and neutralized with 2 mL 1 N HCl solution. Next 80 mL 50% $CaCl_2$ solution was added to this suspension, and the xylan was immediately dissolved. Then water was added to give a total volume 100 mL. The resulting solution was clear with a light-yellow color.

Complexes: Xylan–iodine complex precipitated from saturated iodine without added iodide solution was prepared as follows: a bag of solid iodine was placed in the stock xylan solution just described. As the iodine could penetrate the bag, after 2 days, much blue complex precipitated from the solution and was separated by centrifugation.

Spectra: UV/Vis spectra were recorded with a Perkin–Elmer Lambda 6 spectrophotometer and converted to second-derivative UV/Vis spectra with a utility supplied by the manufacturer. The following parameters were used: width factor 6, number of points 37.

Raman spectra were recorded with Nd:YAG (1064 nm) laser excitation using a Bruker RFS 100 FT Raman system. The samples were placed in NMR tubes.

Acknowledgements

This work was supported in part by the USDA Forest Service.

References

1. Isenberg, H. *Pulp and Paper Microscopy*, 3rd ed.; The Institute of Paper Chemistry: Appleton, 1967; pp 224–234.
2. Graff, J. H. *Color Atlas for Fiber Identification*; The Institute of Paper Chemistry: Appleton, 1940.
3. Graff, J. H. *Paper Trade J.* **1935**, *100*(16), 45–50.
4. Yu, X.; Houtman, C.; Atalla, R. H. *Carbohydr. Res.* **1996**, *292*, 129–141.
5. Gaillard, B. D. E. *Nature* **1961**, *191*, 1295–1296.
6. Morak, A. J.; Thompson, N. S. *Nature* **1965**, *205*, 69.
7. Gaillard, B. D. E. *Nature* **1966**, *212*, 202–203.
8. Gaillard, B. D. E.; Thompson, N. S.; Morak, A. J. *Carbohydr. Res.* **1969**, *11*, 509–515.
9. Gaillard, B. D. E.; Thompson, N. S. *Carbohydr. Res.* **1971**, *18*, 137–146.
10. Cahill, J. E. *Am. Lab.* **1979**, *11*(11), 79–85.
11. Cahill, J. E.; Padera, F. G. *Am. Lab.* **1980**, *12*(4), 101–112.
12. Meyerstein, D.; Treinin, A. *Trans. Faraday Soc.* **1963**, *59*, 1114–1120.
13. Williams, R. M.; Atalla, R. H. *ACS Sympo. Ser.* **1981**, *150*, 317–330.
14. Williams, R. M.; Atalla, R. H. *J. Chem. Soc., Perkin Trans. 2* **1975**, 1155–1161.
15. Angyal, S. J. *Adv. Carbohydr. Chem. Biochem.* **1989**, *47*, 1–43.
16. Richards, R. J.; Willams, D. G. *Carbohydr. Res.* **1970**, *12*, 409–418.
17. Richards, G. F. *Carbohydr. Res.* **1973**, *26*, 409.
18. Parrett, F. W.; Taylor, N. J. *J. Inorg. Nucl. Chem.* **1970**, *32*, 2458–2461.
19. Nour, E. M.; Chen, L. H.; Lanne, J. *J. Phys. Chem.* **1986**, *90*, 2841–2846.
20. Nour, E. M.; Shahada, L. *Spectrochim. Acta* **1989**, *45A*(10), 1033–1035.
21. Mittag, H.; Stegemann, H.; Fullbier, H. *J. Raman Spectrosc.* **1989**, *20*, 251–255.
22. Mizuno, M.; Tanaka, J. *J. Phys. Chem.* **1985**, *85*, 1789–1794.
23. Deplano, P.; Devillanova, F. A.; Ferraro, J. R.; Mercuri, M. L.; Lippolis, V.; Trogu, E. F. *Appl. Spectrosc.* **1994**, *48*(10), 1236–1241.
24. Deplano, P.; Devillanova, F. A.; Ferraro, J. R.; Isala, F.; Lippolis, V.; Mercuri, M. L. *Appl. Spectrosc.* **1992**, *46*(11), 1625–1629.
25. Allen, T. L.; Keefer, R. F. *J. Am. Chem. Soc.* **1955**, *77*, 2957–2960.